

Emission Excitation Spectroscopy in WS₂ Monolayer Encapsulated in Hexagonal BN

M. ZINKIEWICZ^{a,*}, K. NOGAJEWSKI^a, M. BARTOS^b, K. WATANABE^c, T. TANIGUCHI^c,
M. POTEMSKI^{a,b}, A. BABIŃSKI^a AND M.R. MOLAS^a

^aInstitute of Experimental Physics, Faculty of Physics, University of Warsaw,
L. Pasteura 5, PL-02093 Warszawa, Poland

^bLaboratoire National des Champs Magnétiques Intenses, CNRS-UGA-UPS-INSA-EMFL,
25, av. des Martyrs, 38042 Grenoble, France

^cNational Institute for Materials Science, 1-1 Namiki, Tsukuba 305-0044, Japan

Resonant conditions of the Raman scattering in monolayer WS₂ encapsulated in hexagonal BN are investigated using the Raman scattering excitation technique at low temperature ($T = 5$ K). The resonance of the detected signal with the neutral exciton leads to an extremely rich Raman scattering excitation spectrum, which displays also the Raman scattering features not reported so far. Moreover, the intensities of the observed phonon modes are strongly enhanced when the energy difference between the excitation laser and the neutral exciton emission (X^0) is equal to the corresponding phonon energy. The intensity profile of the out-of-plane A_1' phonon mode reflects the Lorentzian lineshape of the X^0 line with the linewidth of about 4 meV, which underlines the outgoing resonance conditions with the X^0 complex.

DOI: [10.12693/APhysPolA.136.624](https://doi.org/10.12693/APhysPolA.136.624)

PACS/topics: tungsten disulphide monolayer, Raman scattering excitation

1. Introduction

The family of two-dimensional (2D) semiconducting transition metal dichalcogenides (S-TMDs) has recently attracted considerable attention thanks to their unique electronic structures and corresponding optical properties [1, 2]. They also transform from indirect- to direct-band-gap when thinned down from the bulk material to the monolayer (ML) limit [3–6]. Their unique properties promise several optoelectronic applications, which motivates studies of electron–phonon interactions in those materials.

One of key observations reported in S-TMDs is a strong enhancement of the Raman scattering signal, when excitation energy is in resonance with excitonic complexes [7–9]. We have recently shown this effect in monolayer WS₂ on Si/SiO₂ substrate introducing the Raman scattering excitation (RSE) technique [10].

Recently, it has been reported that encapsulation of a S-TMD monolayer in hexagonal BN (h-BN) flakes leads to suppression of the inhomogeneous contribution to the linewidths of excitonic complexes resulting in the significantly narrow spectral lines [11, 12]. Consequently, the encapsulation opens new quality in studies of exciton–phonons interaction in S-TMD monolayers as the measured excitonic emission lines in the h-BN-encapsulated samples are much better energetically

separated from each other as compared to the one deposited on the Si/SiO₂ substrates [11]. The qualitative change of the S-TMD monolayers encapsulated in h-BN motivates our study.

In this work we use the RSE technique to h-BN-encapsulated WS₂ monolayer sample at low temperature ($T = 5$ K). Due to the enhancement of the Raman modes intensity in resonance with the neutral exciton (X^0) emission, an extremely rich Raman spectrum was obtained. The intensity profile of A_1' phonon mode reflects the X^0 lineshape, which underlines the outgoing resonance conditions with this complex.

2. Samples and experimental setups

The studied sample is composed of a WS₂ monolayer embedded between h-BN flakes and supported by a bare Si substrate. The structure was obtained by a two-stage polydimethylsiloxane (PDMS)-based [13] mechanical exfoliation of WS₂ and h-BN bulk crystals. The bottom h-BN layer in h-BN/WS₂/h-BN heterostructure was created in the course of non-deterministic exfoliation. The assembly of h-BN/WS₂/h-BN heterostructure was realized via successive dry transfers of WS₂ ML and capping h-BN flake from PDMS stamps onto the bottom h-BN layer.

The RSE measurements were carried out using a dye laser based on Rhodamine 6G with a tunable wavelength range extending from about 571 nm to almost 600 nm. The investigated sample was placed on a cold finger of a continuous flow cryostat mounted on x – y motorized positioners. The excitation light was focused by means of

*corresponding author; e-mail:
malgorzata.zinkiewicz@fuw.edu.pl

a $50\times$ long-working distance objective (NA=0.50) producing a spot of about $1\ \mu\text{m}$ diameter. The signal was collected via the same microscope objective, sent through a 0.5 m-long monochromator, and then detected by a charge-coupled device camera. The excitation power focused on the sample was stabilized at $50\ \mu\text{W}$ by electrooptical modulator during the RSE measurements. The collection time of each spectrum was only 1 s.

3. Experimental results and discussion

Figure 1 shows the intensity of the optical response as a function of excitation energy measured on monolayer WS_2 encapsulated in h-BN in the form of the color-coded map. The presented spectral window covers the energy range that corresponds to the emission of light due to recombination of the neutral exciton (X^0) in the vicinity of so-called A exciton [14]. It can be seen that the line shape of the detected signal significantly depends on the excitation energy. The two regions of excitation energy can

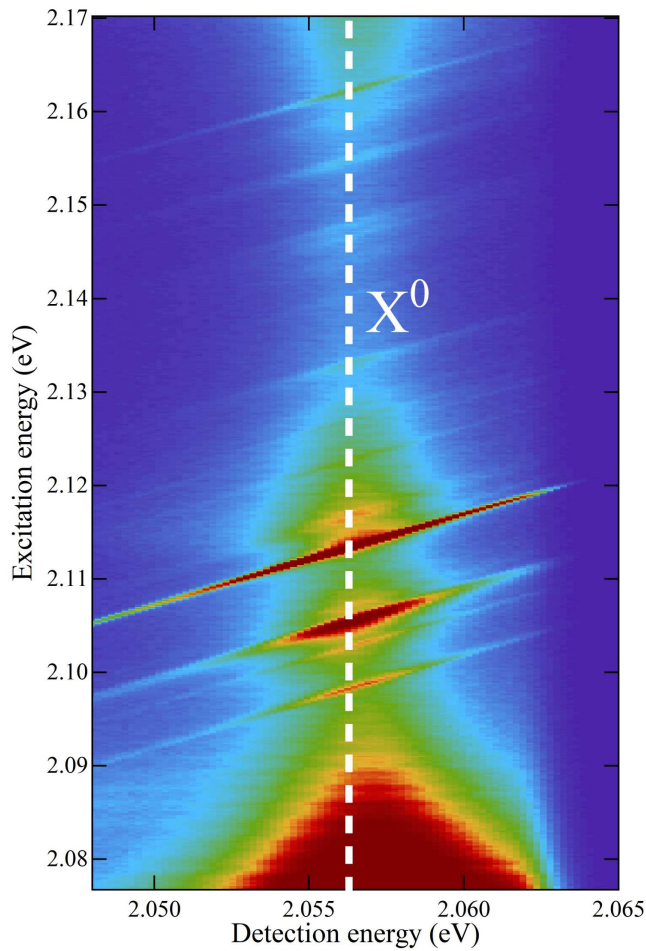


Fig. 1. Optical response of monolayer WS_2 encapsulated in h-BN at $T = 5\ \text{K}$ plotted as a function of excitation energy. The white dashed vertical line denotes the “cross-section” of the map taken at $E = 2.056\ \text{eV}$ (X^0 emission) and presented in Fig. 2.

be clearly distinguished in Fig. 1: (i) $<2.09\ \text{eV}$ in which the emission ascribed to the X^0 is strongly enhanced with decreasing excitation energy, (ii) $>2.09\ \text{eV}$ in which several narrow lines superimposed on the neutral exciton peak are observed. The observed enhancement of the X^0 emission can be described in terms of extremely efficient formation of neutral excitons at higher k -vectors due to the near resonant excitation. Moreover, the narrow emission lines seen in the range (ii) follow the laser excitation energy which points out to the Raman scattering as their origin.

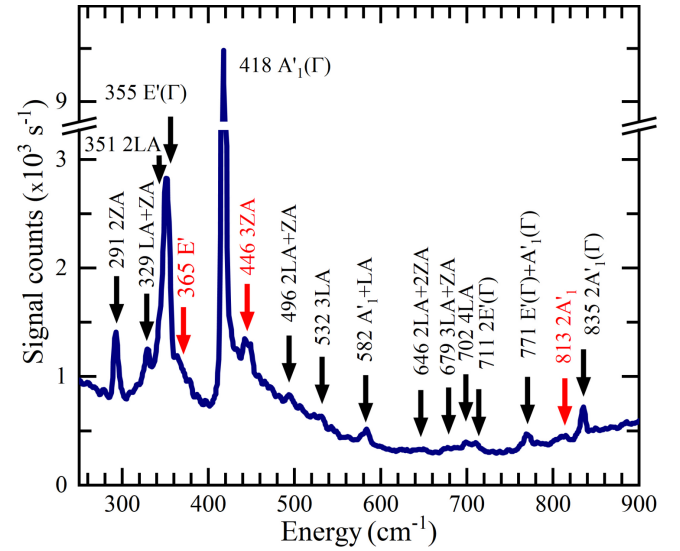


Fig. 2. Low-temperature ($T = 5\ \text{K}$) RSE spectrum of monolayer WS_2 encapsulated in h-BN detected at X^0 energy ($E = 2.056\ \text{eV}$) in the excitation energy range $> 2.09\ \text{eV}$. The horizontal scale represents the Stokes shift between the excitation and detection energies. The assigned peaks correspond to phonons from the M point of the Brillouin zone unless otherwise stated. Features reported in Ref. [10] are marked with black arrows.

In order to study the Raman scattering in the system, we have analyzed its optical response as a function of excitation energy and detected at the neutral exciton energy. The resulting RSE spectrum, displayed as a function of the Stokes shift, is shown in Fig. 2. When interpreting the spectra, it is important to keep in mind that although they correspond to the Raman scattering, they were not obtained at a constant excitation energy, as it is typical for the Raman scattering technique. Due to this resonant condition, i.e., the emitted light in resonance with the neutral exciton, the obtained RSE spectrum displays several Raman scattering peaks including multi-phonon processes. As can be appreciated in Fig. 2, the intensity of the Raman modes are extremely large, e.g., the maximal intensity of the $A_1'(\Gamma)$ (related to the out-of-plane vibrations of sulphur atoms) mode equals 10^5 counts/s. Most of the observed modes have been already reported in Ref. [10]. Moreover, for

two main E' (Γ) and $A'_1(\Gamma)$ phonon modes, long tails of emitted signal at higher energy side are apparent. This is probably due to: (i) the energy dispersion of the E' and A'_1 along the Brillouin zone (BZ). It results in observation of E' (365 cm^{-1}) from the M of BZ, while the corresponding A'_1 expected at 407 cm^{-1} cannot be resolved probably due to the large intensity of the $A'_1(\Gamma)$ peak, (ii) the multi-phonon scattering processes of acoustic phonons accompanying the $A'_1(\Gamma)$ mode, which plays an analogous role as for the enhancement of X^0 emission at the excitation energy $< 2.09\text{ eV}$.

To verify type of the Raman scattering resonance, i.e., incoming or outgoing [15], the intensity profile for the $A'_1(\Gamma)$ mode was determined by fitting of Gaussian function to the emitted signal as a function of tuned laser energy, shown in Fig. 1. Figure 3 presents the integrated intensity Raman profile of the out-of-plane A'_1 phonon mode versus its energy. As can be noted, the shape of the A'_1 enhancement can be described by the Lorentzian function with energy of about 2.057 eV and the width of around 3.8 meV . This shape well corresponds to the shape of the X^0 emission (see Fig. 3), which also can be characterized by the Lorentzian profile with set of parameters: energy and width on the order of 2.056 eV and 4.1 meV , respectively. As the intensity profile of the A'_1 mode reflects the X^0 line shape and the maximum A'_1 enhancement takes place when the energy difference between the excitation and the neutral exciton, it indicates the outgoing character of the apparent resonant conditions.

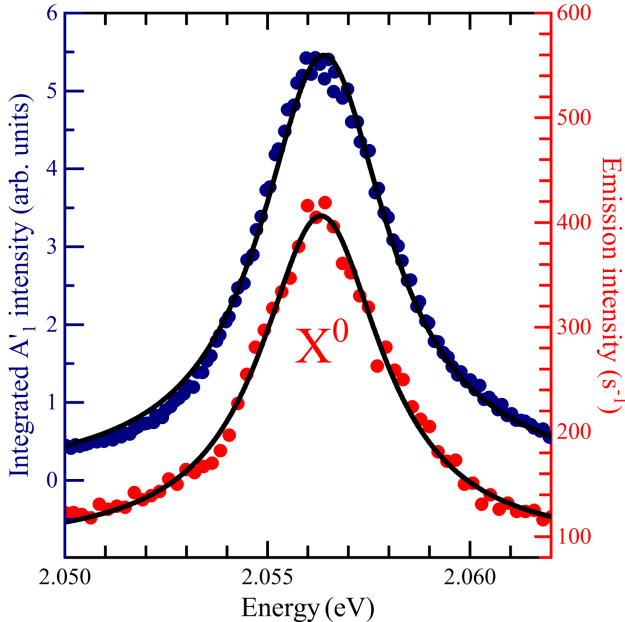


Fig. 3. The integrated intensity Raman profile of the out-of-plane A'_1 phonon mode (blue points) and the photoluminescence signal of the X^0 emission line under excitation of E in eV (red points). The colour solid lines correspond to the selected data taken from Fig. 1.

4. Conclusions

We have presented a study of low-temperature photoluminescence excitation performed on WS_2 monolayer encapsulated in h-BN. The resonant conditions of the Raman scattering found with the neutral exciton emission give rise to an extremely rich Raman scattering excitation spectrum. Due to the obtained intensity profile of the A'_1 phonon mode reflecting of the X^0 line shape, the observed enhancement of the phonon mode originates from the outgoing resonance conditions.

Acknowledgments

The work has been supported by the National Science Centre, Poland (grants no. 2017/24/C/ST3/00119, 2017/27/B/ST3/00205) and the EU Graphene Flagship project (no. 785219), the ATOMOPTO project (TEAM programme of the Foundation for Polish Science, co-financed by the EU within the ERD-Fund). K.W. and T.T. acknowledge support from the Elemental Strategy Initiative conducted by the MEXT, Japan, and the CREST (JPMJCR15F3), JST.

References

- [1] M. Koperski, M.R. Molas, A. Arora, K. Nogajewski, A. Slobodeniuk, C. Faugeras, M. Potemski, *Nanophotonics* **6**, 1289 (2017).
- [2] G. Wang, A. Chernikov, M.M. Glazov, T.F. Heinz, X. Marie, T. Amand, B. Urbaszek, *Rev. Mod. Phys.* **90**, 021001 (2018).
- [3] K.F. Mak, C. Lee, J. Hone, J. Shan, T.F. Heinz, *Phys. Rev. Lett.* **105**, 136805 (2010).
- [4] A. Arora, M. Koperski, K. Nogajewski, J. Marcus, C. Faugeras, M. Potemski, *Nanoscale* **7**, 10421 (2015).
- [5] A. Arora, K. Nogajewski, M. Molas, M. Koperski, M. Potemski, *Nanoscale* **7**, 20769 (2015).
- [6] M.R. Molas, K. Nogajewski, A.O. Slobodeniuk, J. Binder, M. Bartos, M. Potemski, *Nanoscale* **9**, 13128 (2017).
- [7] K. Gołasa, M. Grzeszczyk, P. Leszczyński, C. Faugeras, A.A.L. Nicolet, A. Wysmołek, M. Potemski, A. Babiński, *Appl. Phys. Lett.* **104**, 092106 (2014).
- [8] M. Grzeszczyk, K. Gołasa, M. Zinkiewicz, K. Nogajewski, M.R. Molas, M. Potemski, A. Wysmołek, A. Babiński, *2D Materials* **3**, 025010 (2016).
- [9] M. Grzeszczyk, K. Gołasa, M.R. Molas, K. Nogajewski, M. Zinkiewicz, M. Potemski, A. Wysmołek, A. Babiński, *Sci. Rep.* **8**, 17745 (2018).
- [10] M.R. Molas, K. Nogajewski, M. Potemski, A. Babiński, *Sci. Rep.* **7**, 5036 (2017).
- [11] F. Cadiz, E. Courtade, C. Robert, G. Wang, Y. Shen, H. Cai, T. Taniguchi, K. Watanabe, H. Carrere, D. Lagarde, M. Manca, T. Amand, P. Renucci, S. Tongay, X. Marie, B. Urbaszek, *Phys. Rev. X* **7**, 021026 (2017).

- [12] J. Wierzbowski, J. Klein, F. Sigger, C. Straubinger, M. Kremser, T. Taniguchi, K. Watanabe, U. Wurstbauer, A.W. Holleitner, M. Kaniber, K. Müller, J.J. Finley, *Sci. Rep.* **7**, 12383 (2017).
- [13] A. Castellanos-Gomez, M. Buscema, R. Molenaar, V. Singh, L. Janssen, H.S.J. van der Zant, G.A. Steele, *2D Materials* **1**, 011002 (2014).
- [14] D. Vaclavkova, J. Wyzula, K. Nogajewski, M. Bartos, A.O. Slobodeniuk, C. Faugeras, M. Potemski, M.R. Molas, *Nanotechnology* **29**, 325705 (2018).
- [15] L. Viña, J.M. Calleja, A. Cros, A. Cantarero, T. Berendschot, J.A.A.J. Perenboom, K. Ploog, *Phys. Rev. B* **53**, 3975 (1996).